Available online at www.sciencedirect.com

ScienceDirect

Procedia Engineering 199 (2017) 3164–3169

Procedia Engineering

www.elsevier.com/locate/procedia

X International Conference on Structural Dynamics, EURODYN 2017

Dry galloping in inclined cables: linear stability analysis

Giuseppe Piccardo[b], Daniele Zulli[a,*], Angelo Luongo[a]

[a]*M&MOCS, International Research Center on Mathematics and Mechanics of Complex Systems, University of L'Aquila, Italy*
[b]*DICCA, Department of Civil, Chemical and Environmental Engineering Department, University of Genoa, Italy*

Abstract

In the last decade, dry galloping has been frequently observed on real stay cables also in the case of circular cross section. It is an aeroelastic phenomenon which occurs when structures or structural elements are generically placed with respect to the wind, being both incidence and yaw angles different from zero. Here, after writing down the equations which describe the static reference configuration of an inclined cable under the self-weight, the equations of motion are obtained up to third order, where the forces related to the wind are evaluated coherently with an aerodynamic model, drawn under the quasi-steady hypothesis. A Galerkin projection is carried out and the critical conditions causing Hopf bifurcation on the trivial equilibium configuration are then evaluated.

Peer-review under responsibility of the organizing committee of EURODYN 2017.

Keywords: Dry galloping; inclined cable; bifurcation; stability; quasi-steady modeling; yawed cylinders

1. Introduction

Stay-cables are structural members with low weight-to-stiffness ratio, which are typically used in important engineering structures like bridges and towers. In the literature many analytical formulations have been proposed so far. In [1] the free dynamics of low-inclined stay-cables is analyzed suitably modifying the equations valid for horizontally supported cables, after the application of a rotation of the coordinate system and making it to lay on the inclined chord. In [2] inclined cables are considered in the linear field, and an asymptotic expression for natural frequencies and modal shapes is proposed, showing hybrid features as well as frequency avoiding in certain narrow ranges of parameters. In [3], a nonlinear model of flexible inclined cables is introduced and then, after evaluation of the order of magnitude of some terms, simplifications are suggested. Effects of wind on cables have been considered in numerous studies, mainly based on simplified aerodynamic principles (e.g., [4]). A section model suitable to the study of the critical and post-critical conditions of an internally resonant system under steady wind is proposed in [5–7]. In [8–10], a consistent model of beam-like cable is introduced to take into account the effect of the twist and bending in horizontally supported cables with iced cross section. In [11], harmonic base motion and instability due to the presence of a rain rivulet on the cross section are concurrently considered on a stay-cable, with the aim to study possible interaction

* Corresponding author. Tel.: +39-0862-434537 ; fax: +39-0862-434548.
E-mail address: daniele.zulli@univaq.it

1877-7058
Peer-review under responsibility of the organizing committee of EURODYN 2017.
10.1016/j.proeng.2017.09.508

phenomena. In [12] sagged inclined cables plunged in viscous fluid are considered and, after discussing the static configuration, eigenfrequencies and modal damping factors are evaluated through a Galerkin approach. Galloping-like phenomena in circular cylinder occurring in case of presence of yaw angle has been recently observed (e.g., [13]), and the mechanism inducing this kind of instability has been extensively analyzed by means of wind tunnel tests. Despite unsteadiness and spatial variation of the flow can be significant during the cable motion, an approximate description of dry galloping through a quasi-steady model has been proposed (e.g., [14]). In [15], the stability of a sectional model of inclined cable under yawed wind is analytically addressed through a two d.o.f. system, after rigorous formulation of the aerodynamic model. In the present paper, starting from the nonlinear elastic model proposed in [3] and the aerodynamic model proposed in [15], the analysis of galloping-like instability in yawed conditions is performed on a full-scale inclined stay. Natural frequencies and normal modes are numerically obtained, taking into account the possible significant variation along the span of both the curvature and the pre-stress already in the static configuration. Then, after a Galerkin projection of the partial differential equations on the first significant modes, the stability of the trivial solution under the effect of the yawed steady wind is addressed, in order to get information on the triggering of dry galloping.

2. Mechanical model

2.1. The static configuration

It is well-established that the configuration of cables having length greater then the chord span and under the action of self-weight can be suitably analyzed in the hypothesis of inextensible material [12]. Thus, the static configuration of a stay-cable, considered as non polar continuum, with fixed supports and under the action of self-weight, is described by the inextensible catenary, which is solution of the equilibrium equations [11]. It represents the reference configuration for the dynamic incremental model. With reference to Fig. 1a, indicating with $\bar{x}$ and $\bar{y}$ the horizontal and vertical components of the position $\bar{\mathbf{x}}$ of the axis line of the cable at abscissa s, respectively, the inextensible catenary is:

$$\bar{x}(s) = \frac{H}{mg}\Big[\arcsin\Big(\frac{mgs}{H} + c\Big) - \arcsin(c)\Big], \quad \bar{y}(s) = \frac{H}{mg}\Big[\sqrt{1 + \Big(\frac{mgs}{H} + c\Big)^2} - \sqrt{1 + c^2}\Big] \tag{1}$$

where H is the (constant) horizontal component of the pre-stress, m the mass linear density, g the gravity acceleration and c a constant. Imposing the boundary conditions $\bar{x}(l) = x_l$ and $\bar{y}(l) = y_l$, i.e. choosing the position of the right support located at abscissa $s = l$, which is the length of the cable, one can numerically evaluate H and c, and therefore fully know the initial configuration by means of Eqs. (1). Then, evaluation of the angle $\bar{\vartheta}$ of the tangent vector to the axis line $\bar{\mathbf{a}}_1$ with respect to the horizontal axis is easily obtained: $\tan\bar{\vartheta}(s) = \frac{mgs}{H} + c$, and consequently the curvature of the cable is $\bar{\kappa}(s) = \bar{\vartheta}'(s)$, where prime stands for differentiation with respect to s. Finally, the cable pre-stress is $\bar{T}(s) = \frac{H}{\cos(\bar{\vartheta}(s))}$. The unitary vector $\bar{\mathbf{a}}_1$, with the orthogonal unitary vector $\bar{\mathbf{a}}_2$ lying on the vertical plane and a third, out of plane vector $\bar{\mathbf{a}}_3 = \bar{\mathbf{a}}_1 \times \bar{\mathbf{a}}_2$, define a basis for the vector space of the configurations. It is worth noticing that, if the approximation of uniform curvature and pre-stress is reliable for horizontal taut cables, on the other hand, in cases of inclined or moderately slack cables, the variation of $\bar{\kappa}(s)$ and $\bar{T}(s)$ with s can be considerable, and the hypothesis of considering both of them as uniform along the cable can lead to significant differences. With the aim of considering a model valid for several possible configurations of inclined cable, from very taut to very slack, here the dependence of both $\bar{\kappa}(s)$ and $\bar{T}(s)$ on s is preserved.

2.2. The incremental equations of motion

The incremental load vector $\tilde{\mathbf{b}}$, which includes aeroelastic forces, is applied to the cable in the reference configuration. In order to evaluate the related effects, in general, it is obviously essential to consider extensional material from now on; in particular, an axial stiffness EA is introduced in order to rely to linear elastic material, such that the response law is $T(s) = EA\varepsilon(s)$, where $T(s)$ is the dynamic increment of longitudinal stress and $\varepsilon(s)$ is the nonlinear strain of the cable. The current time-dependent position $\mathbf{x}$ of the cable is obtained by means of a (time-dependent) displacement $\mathbf{u}$ from the reference position $\bar{\mathbf{x}}$, namely $\mathbf{x} = \bar{\mathbf{x}} + \mathbf{u}$, where the unknown components of the displacement vector on the basis $(\bar{\mathbf{a}}_1, \bar{\mathbf{a}}_2, \bar{\mathbf{a}}_3)$ are $[\mathbf{u}] = [u(s), v(s), w(s)]^T$. The expression of the strain measure in terms of components of $\mathbf{u}$

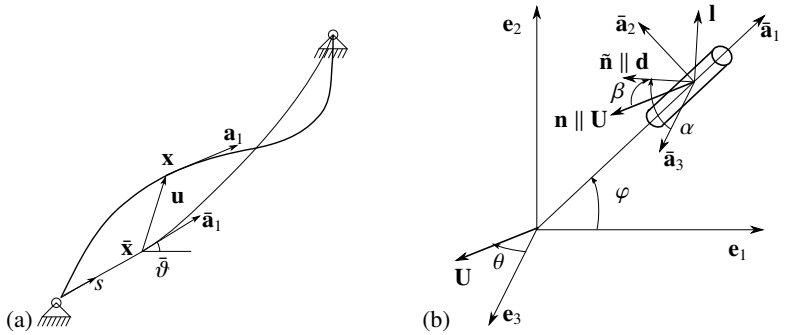

Figure 1: (a) Static position $\bar{\mathbf{x}}$ and current position $\mathbf{x}$ of the axis line, with respective tangent vectors $\bar{\mathbf{a}}_1$ and $\mathbf{a}_1$. (b) Wind velocity and its projection on the plane of the cross section, defining the angles α and β.

is easily obtained (see [3]) as $\varepsilon(s) = \sqrt{(1 + u' + \bar{\kappa}v)^2 + (v' + \bar{\kappa}u)^2 + w'^2} - 1$, and the vector form of the equations of motion turns out to be

$$[(\bar{T} + EA\varepsilon)\mathbf{a}_1]' - \bar{T}'\bar{\mathbf{a}}_1 - \bar{T}\bar{\kappa}\bar{\mathbf{a}}_2 + \tilde{\mathbf{b}} = m\ddot{\mathbf{u}}(s) \tag{2}$$

where $\mathbf{a}_1$ is the (unknown) tangent vector to the current configuration of the axis line, whose expression is $\mathbf{a}_1 = \frac{1}{1+\varepsilon}(\bar{\mathbf{a}}_1 + \mathbf{u}')$ and the dot stands for time differentiation. After introducing the approximation $\mathbf{a}_1 \simeq (\bar{\mathbf{a}}_1 + \mathbf{u}')$ and the application of the static condensation of the longitudinal displacement, which is consequence of the much higher celerity of the longitudinal waves with respect to the transverse ones, the following form of the equations of motion in terms of the components v, w up to the third order is obtained:

$$\begin{aligned} &\ddot{v} + c_v\dot{v} - (\tau v')' - \frac{\kappa\varepsilon}{\gamma} - 2\frac{\kappa\varepsilon^2}{\gamma} - \kappa^2\varepsilon v - 2\frac{\kappa\varepsilon\tau}{\gamma} - \kappa^2\tau v + \gamma\kappa(\tau + \varepsilon)(v'^2 + w'^2) - \varepsilon v'' + b_2 = 0 \\ &\ddot{w} + c_w\dot{w} - (\tau w')' - \varepsilon w'' + b_3 = 0 \qquad\qquad \text{where} \qquad \varepsilon = -\gamma\int_0^1 kv\,ds + \frac{\gamma^2}{2}\int_0^1 (v'^2 + w'^2)ds \end{aligned} \tag{3}$$

and terms of higher power than the third, induced by the square of ε or its product with nonlinear terms, can be neglected. Equations (3) are written in nondimensional form, after the definition of the following terms:

$$\tilde{s} = \frac{s}{l}, \quad \tilde{t} = \omega t, \quad (\tilde{v}, \tilde{w}) = \frac{(v, w)}{\eta}, \quad \kappa = \bar{\kappa}l, \quad \tau = \frac{\bar{T}}{EA}, \quad \gamma = \frac{\eta}{l}, \quad (\tilde{b}_v, \tilde{b}_w) = \frac{(b_v, b_w)}{m\omega^2\eta}, \quad \omega = \frac{1}{l}\sqrt{\frac{EA}{m}} \tag{4}$$

with η the sag of the cable in the static configuration (evaluated where the tangent vector to the axis line is parallel to the chord), b_v, b_w being the components of $\mathbf{b}$ along $\bar{\mathbf{a}}_2, \bar{\mathbf{a}}_3$, and omitting the tilde. Boundary conditions read: $v(0) = w(0) = v(1) = w(1) = 0$.

3. Aerodynamic model

Aerodynamic forces are defined in the framework of the quasi-steady theory, i.e. under the hypothesis of much faster time-scale of the fluid oscillations in the wake of the cylinder with respect to that of the oscillations of the cylinder itself. The main physical aspect behind the aerodynamic model is that, nevertheless the cross section of the cylinder is circular, the existence of a yaw angle lets the wind blow in a direction such that the cross section appears to it as no more circular but elliptical, giving rise to a lift component of the force. With reference to [15] and to Fig. 1b, the aerodynamic force is first evaluated considering a fixed cylinder, in order to relate all the relevant terms to the angles defined in the experimental static test described in [14]. Then, the expression will be modified taking into account a relative velocity of the cylinder with respect to the fluid, as typically done in the quasi-steady theory; consequently, the modified angles will be expressed in terms of the angles defined in the case of fixed cylinder. Aerodynamic forces can be conveniently expressed in the Frenet triad (e.g.,[16]). The circular cylinder is locally aligned with the axes $(\bar{\mathbf{a}}_1, \bar{\mathbf{a}}_2, \bar{\mathbf{a}}_3)$, where $\bar{\mathbf{a}}_1$ is tangent to the axis line and is inclined of an angle φ with respect to the horizontal axis $\mathbf{e}_1$, and

$(\bar{\mathbf{a}}_2, \bar{\mathbf{a}}_3)$ lie on the cross section. Note that the plane spanned by $(\bar{\mathbf{a}}_2, \bar{\mathbf{a}}_3$ is vertical and coincides with the one spanned by $\mathbf{e}_1, \mathbf{e}_2$; furthermore, φ is approximately close to the inclination of the chord of the cable. The wind blows with velocity $\mathbf{U}$ along a direction indicated as $\mathbf{n} := \mathbf{U}/\|\mathbf{U}\|$, which lies on the horizontal plane $(\mathbf{e}_1, \mathbf{e}_3)$. The direction $\mathbf{n}$ is inclined of θ with respect to $\mathbf{e}_3$, and is not perpendicular to the axis $\bar{\mathbf{a}}_1$. The direction of the wind $\mathbf{n}$ is projected on the plane $(\bar{\mathbf{a}}_2, \bar{\mathbf{a}}_3)$ of the cross section, giving rise to the vector $\tilde{\mathbf{n}}$ and defining the yaw angle β. Moreover, the vector $\tilde{\mathbf{n}}$ defines the attack angle α with respect to $\bar{\mathbf{a}}_3$. It can be easily show (see [15] for the details) that $\tan\alpha = \tan\theta \sin\varphi$ and $\sin\beta = \sin\theta\cos\varphi$. Neglecting the component of the force along the $\bar{\mathbf{a}}_1$ direction, the vector of the aerodynamic force reads:

$$\mathbf{b} = \frac{1}{2}\rho b \|\mathbf{U}\|^2 (c_d \mathbf{d} + c_l \mathbf{l}) \tag{5}$$

where ρ is the air density, b is a characteristic dimension of the cross section (namely the diameter), $\mathbf{d}$ is the direction of the drag, defined as $\mathbf{d} = \tilde{\mathbf{n}}/\|\tilde{\mathbf{n}}\|$, $\mathbf{l}$ defines the lift direction ($\mathbf{l} = \mathbf{d} \times \bar{\mathbf{a}}_1$), and c_d and c_l are the drag and lift coefficients, respectively. In particular, the drag and lift coefficients in Eq. (5) depend on β but are independent of α, due to the polar symmetry of the cross section; moreover their dependence on the wind velocity through the Reynolds number Re can be considered as slow (plots of their evolution in certain ranges of β and Re are shown in [15]). On the other hand, α appears in the definition of $\mathbf{d}$ and $\mathbf{l}$. Some algebraic manipulations not described here allow one to equivalently write Eq. (5) in the following form:

$$\mathbf{b} = \frac{1}{2}\rho b \frac{\|\mathbf{U}\|^2}{\cos\beta} \mathbf{C}(\beta)\mathbf{n}(\alpha,\beta) \qquad \text{where} \qquad [\mathbf{C}(\beta)] = \begin{bmatrix} 0 & 0 & 0 \\ 0 & c_d(\beta) & -c_l(\beta) \\ 0 & c_l(\beta) & c_d(\beta) \end{bmatrix}, \qquad [\mathbf{n}(\alpha,\beta)] = \begin{bmatrix} -\sin\beta \\ \cos\beta\sin\alpha \\ \cos\beta\cos\alpha \end{bmatrix} \tag{6}$$

being $\mathbf{C}(\beta)$ and $\mathbf{n}(\alpha,\beta)$ described on the base $(\bar{\mathbf{a}}_j)$. As a second step, the relative velocity between wind flow and cylinder $\mathbf{U}^* = \mathbf{U} - \dot{\mathbf{u}}$ is considered instead of $\mathbf{U}$, entailing a redefinition of the involved angles. If $\mathbf{z} := -\dot{\mathbf{u}}/\|\mathbf{U}\|$, then the relative velocity becomes $\mathbf{U}^* = \|\mathbf{U}\|(\mathbf{n}+\mathbf{z})$, and its direction is indicated as $\mathbf{n}^* = (\mathbf{n}+\mathbf{z})/\|\mathbf{n}+\mathbf{z}\|$, which is generally no more lying on a horizontal plane, however the instantaneous yaw angle is $\beta^* = -\arcsin(\mathbf{n}^* \cdot \bar{\mathbf{a}}_1)$, where the dot stands for scalar product. Note that β^* depends on $\mathbf{z}$. Substituting in Eq. (6) the term $\mathbf{U}$, $\mathbf{n}$, β with the instantaneous relevant terms $\mathbf{U}^*$, $\mathbf{n}^*$, β^*, the following expression for the aerodynamic force is obtained:

$$\mathbf{b} = \frac{1}{2}\rho b \frac{\|\mathbf{U}\|^2}{\cos\beta^*} \|\mathbf{n}+\mathbf{z}\| \mathbf{C}(\beta^*)(\mathbf{n}(\alpha,\beta)+\mathbf{z}) \tag{7}$$

A Taylor expansion of Eq. (7) up to the third order in $\mathbf{z}$ is done, neglecting the contribution of the longitudinal velocity $\dot{u}$, consistently with the kinematic condensation process. It provides the following expressions for the components of the aerodynamic force along $\bar{\mathbf{a}}_2$ and $\bar{\mathbf{a}}_3$, respectively:

$$b_j = c_{j0} + c_{jv}\dot{v} + c_{jvv}\dot{v}^2 + c_{jvvv}\dot{v}^3 + c_{jw}\dot{w} + c_{jww}\dot{w}^2 + c_{jwww}\dot{w}^3 + c_{jvw}\dot{v}\dot{w} + c_{jvvw}\dot{v}^2\dot{w} + c_{jvww}\dot{v}\dot{w}^2 \tag{8}$$

for $j = 2, 3$. Expressions of coefficients $c_j(\|\mathbf{U}\|, \alpha, \beta)$ are not reported here for the sake of brevity.

In general, it is well-known that wind profiles are significantly dependent on the height above the ground. Therefore, dealing with inclined cables which can easily span for several hundreds of meters above the ground, it would be reasonable to take into account modification of the wind velocity with the abscissa s. However in this work, with favor of safety and simplicity, a uniform velocity is applied along the cable, obtained as an amplification of the wind design reference velocity V by the mean wind velocity profile coefficient $k_v(s)$ as provided by codes and guidelines (e.g., CNR DT 207_2008) and evaluated at the half span of the cable ($s = 1/2$), namely $\|\mathbf{U}\| = k_v(1/2)V$.

4. Stability analysis

The partial differential equations of motion (3), with the forcing terms defined in (8), are addressed using a Galerkin approach by means of the first linear modes, the latter obtained from the associated linear Hamiltonian problem. In particular, if $\psi_{v_j}(s)$ and $\psi_{w_k}(s)$, $j = 1, \ldots, n$, $k = 1, \ldots, m$ are the first in-plane and out-of-plane eigenfunctions, respectively, and defining the unknown modal amplitudes $q_j^i(t)$ for in-plane and $q_k^o(t)$ for out-of-plane modes, then:

$$\begin{Bmatrix} v(s,t) \\ w(s,t) \end{Bmatrix} = \sum_{j=1}^{n} q_j^i(t) \begin{Bmatrix} \psi_{v_j}(s) \\ 0 \end{Bmatrix} + \sum_{k=1}^{m} q_k^o(t) \begin{Bmatrix} 0 \\ \psi_{w_k}(s) \end{Bmatrix} \tag{9}$$

Substituting Eq. (9) in Eq. (3) and multiplying each equation for δv, δw, respectively (where δ is the variation symbol), integrating for $s \in [0, 1]$, summing and collecting the terms which multiply δq_j^i and δq_k^o, the following reduced model is obtained:

$$\mathbf{M}\ddot{\mathbf{q}} + \mathbf{C}\dot{\mathbf{q}} + \mathbf{K}\mathbf{q} + \mathbf{n}_2(\mathbf{q},\mathbf{q}) + \mathring{\mathbf{n}}_2(\dot{\mathbf{q}},\dot{\mathbf{q}}) + \mathbf{n}_3(\mathbf{q},\mathbf{q},\mathbf{q}) + \mathring{\mathbf{n}}_3(\dot{\mathbf{q}},\dot{\mathbf{q}},\dot{\mathbf{q}}) + \mathring{\mathbf{n}}_0 = \mathbf{0} \tag{10}$$

where $\mathbf{q} = (q_j^i, q_k^o)$ is the $m+n$-vector of the Lagrangian parameters, and $\mathbf{M}$, $\mathbf{C}$, $\mathbf{K}$ are the mass, damping (structural plus aerodynamic), stiffness matrices, respectively; moreover $\mathbf{n}_2, \mathbf{n}_3$ are nonlinear quadratic and cubic elastic operators, $\mathring{\mathbf{n}}_0$ is a constant aerodynamic vector and $\mathring{\mathbf{n}}_2, \mathring{\mathbf{n}}_3$ are nonlinear quadratic and cubic aerodynamic operators. First, the constant term is tentatively neglected and, consequently, stability analysis of the trivial solution is performed, in order to search for the critical wind velocity which triggers a Hopf bifurcation, occurring when one eigenvalue passes from left to right the imaginary axis of the Gauss plane and all the other eigenvalues have negative real parts. This is done solving the relevant eigenvalue problem which reads $[\lambda^2\mathbf{M} + \lambda\mathbf{C} + \mathbf{K}]\boldsymbol{\varphi} = \mathbf{0}$.

5. Numerical results

A full-scale stay-cable with the following mechanical and geometrical properties is considered for the analysis, corresponding to a wind-tunnel test showing galloping-like instability (case 2C in [14]): the chord is inclined of $\varphi = 45^o$ and its length is 700 m. The length of the cable in the static configuration is $l = 703.5$ m, the mass per unit-length is $m = 60.8$ kg/m, the diameter of the cross section is $b = 0.16$ m, the elastic modulus is $E = 2.1 \times 10^5$ MPa, the structural damping ratio is $\xi = 0.08\%$ for each mode. About the aerodynamic parameters, $\rho = 1.25$ kg/m^3, $\beta = 30^o$, $\alpha = 35.3^o$ (which correspond to a wind vector inclined in the horizontal plane of $\theta = 45^o$ with respect to $\mathbf{e}_3$, see Fig. 1b), $k_v(1/2) = 1.6$. The corresponding static configuration is shown in Fig. 2a, while the non-dimensional static pre-stress τ and curvature κ are shown as function of s in Figure 2b, showing a not negligible variation along the span, especially in κ. First two in-plane modes and out-of-plane modes are shown in Figure 2c, numerically evaluated using a polynomial collocation method [17]. Non-dimensional natural frequencies are $\omega_{w_1} = 0.045$, $\omega_{w_2} = 0.090$ for out-of-plane modes and $\omega_{v_1} = 0.088$, $\omega_{v_2} = 0.127$ for in-plane modes: note that the unique internal resonance condition is the classical one involving the in-plane and out-of-plane anti-symmetric modes, in ratio 1:1. First, single d.o.f. models are considered, involving alternatively one of the modes shown in Fig. 2c: the real part of the eigenvalues is shown in Fig. 3a as a function of the wind reference velocity V. Note that, in this cases, in-plane modes have smaller critical velocity, $V_{cr} \simeq 16.1$ m/s (black circle in Fig. 3a), than that of out-of-plane modes, $V_{cr} \simeq 16.8$ m/s (black box in Fig. 3a); however the two velocities are fairly close, due to the effective orientation of the lift direction, which has large components on both $\bar{\mathbf{a}}_2$ and $\bar{\mathbf{a}}_3$. This fact induces the expectation of occurrence of multiple Hopf bifurcations when considering more-than-one d.o.f. systems. In particular, when considering two or three d.o.f. systems involving just mistuned modes (i.e. not concurrently involving ψ_{v_1} and ψ_{w_2}) no modification is detected in the evolution of the eigenvalues with respect to the wind velocity compared to the cases of single d.o.f. systems. On the other hand, a completely different behavior is detected when considering the two internally resonant modes, even in a two d.o.f. system of type (ψ_{v_1}, ψ_{w_2}): the real part of the relevant eigenvalues is shown in Fig. 3b, which is modified compared to the single d.o.f. systems, highlighting a significant interaction between the two d.o.f. which gives rise to a reduction of the critical velocity to $V_{cr} = 15.7$ m/s; the other eigenvalue is always stable. The same behavior is preserved when dealing with system with three or four d.o.f., provided the presence of the two resonant modes which show that the interaction between them is dominant with respect to the determination of the critical condition. The corresponding critical eigenvalue in Fig. 3c shows coupling between the v and w components, mainly in the real part.

6. Conclusions

A dynamic model of inclined full-scale stay-cables under the effect of yawed steady wind, which is able to induce dry galloping, is proposed. The static configuration is shown and used as reference for the dynamic displacement. The equations of motion are written, taking into account the variation of both the pre-stress and the initial curvature along the span. The aerodynamic model is taken from the literature and adapted to a full-scale cable. A Galerkin approach is applied and discussion on the stability of the trivial solution is done in case of almost mistuned natural frequencies. In particular, reduced models concurrently considering the in-plane and out-of-plane anti-symmetric modes, which turn

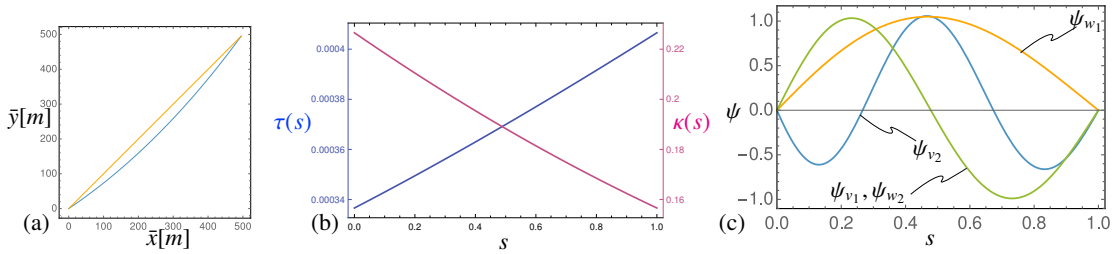

Figure 2: (a) Static configuration (in blue), with inclined chord (in orange); (b) non-dimensional static pre-stress τ (in blue), and curvature κ (in magenta) as function of s; (c) in-plane modes: first (green) and second (blue), and out-of-plane modes: first (orange) and second (green).

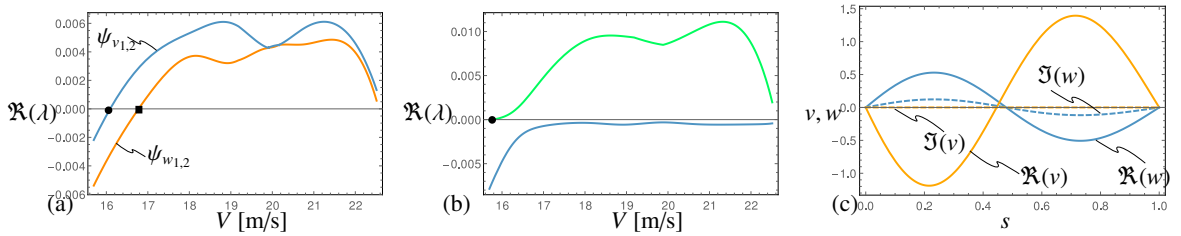

Figure 3: (a) Critical eigenvalues for single d.o.f. systems: in-plane models (in blue), out-of-plane models (in orange); (b) critical (in green) and non-critical (in blue) eigenvalues for a two d.o.f. system with in-plane and out-of-plane anti-symmetric modes. (c) real (continuous line) and imaginary (dashed lines) parts of the v (in orange) and w (in blue) components of critical mode for the two d.o.f. system with anti-symmetric modes.

out to be the sole modes in internal resonance, involve interaction between the modes giving rise to critical velocities smaller than those of the corresponding single d.o.f. systems.

References

[1] H. Irvine, Cable structures, MiT Press, Cambridge, Mass., 1981.
[2] M. Triantafyllou, L. Grinfogel, Natural frequencies and modes of inclined cables, J. Struct. Eng. 112 (1986) 139–148.
[3] A. Luongo, D. Zulli, Mathematical Models of Beams and Cables, Iste - Wiley, 2013.
[4] R. Blevins, Flow-induced Vibration, second ed., Krieger Publishing Company, Florida, 2001.
[5] A. Luongo, G. Piccardo, Linear instability mechanisms for coupled translational galloping, J. Sound Vib. 288 (2005) 1027–1047.
[6] G. Piccardo, A methodology for the study of coupled aeroelastic phenomena, J. Wind Eng. 98 (1993) 241–252.
[7] G. Piccardo, L. Pagnini, F. Tubino, Some research perspectives in galloping phenomena: critical conditions and post-critical behavior, Contin. Mech. Thermodyn. 27 (2017) 261–285.
[8] A. Luongo, D. Zulli, G. Piccardo, A linear curved-beam model for the analysis of galloping in suspended cables, J. Mech. Mater. Struct. 2 (2007) 675–694.
[9] A. Luongo, D. Zulli, G. Piccardo, Analytical and numerical approaches to nonlinear galloping of internally resonant suspended cables, J. Sound Vib. 315 (2008) 375–393.
[10] A. Luongo, D. Zulli, G. Piccardo, On the effect of twist angle on nonlinear galloping of suspended cables, Comp. Struct. 87 (2009) 1003–1014.
[11] A. Luongo, Zulli, Dynamic instability of inclined cables under combined wind flow and support motion, Nonlinear Dyn. 67 (2012) 71–87.
[12] S. Sorokin, G. Rega, On modelling and linear vibrations of arbitrarily sagged inclined cables in a quiescent viscous fluid, J. Fluids Struct. 23 (2007) 1077–1092.
[13] J. Macdonald, G. Larose, Two-degree-of-freedom inclined cable galloping - Part 1: General formulation and solution for perfectly tuned system, J. Wind Eng. Ind. Aerodyn. 96 (2008) 291–307.
[14] S. Cheng, G. L. Larose, M. G. Savage, H. Tanaka, P. A. Irwin, Experimental study on the wind-induced vibration of a dry inclined cablepart i: Phenomena, J. Wind Eng. Ind. Aerodyn. 96 (2008) 2231 – 2253.
[15] L. Carassale, A. Freda, G. Piccardo, Aeroelastic forces on yawed circular cylinders: quasi-steady modeling and aerodynamic instability, Wind Struct. 8 (2005) 373–388.
[16] A. Luongo, G. Piccardo, Non-linear galloping of sagged cables in 1:2 internal resonance, J. Sound Vib. 214 (1998) 915–940.
[17] G. Kitzhofer, O. Koch, G. Pulverer, C. Simon, E. Weinmüller, BVPSUITE, A New MATLAB Solver for Singular Implicit Boundary Value Problems, Technical Report 35, Institute for Analysis and Scientific Computing - TU, Wien, 2009.